optica

Direct control of mode-locking states of a fiber laser

R. Iegorov,[1,2,†] T. Teamir,[1,†] G. Makey,[1] and F. Ö. Ilday[1,2,*]

[1]Department of Physics, Bilkent University, 06800 Ankara, Turkey
[2]Department of Electrical and Electronics Engineering, Bilkent University, Ankara 06800, Turkey
*Corresponding author: ilday@bilkent.edu.tr

Mode locking is a non-equilibrium steady state. Capability to control mode-locking states can be used to improve performance as well as shed light on non-equilibrium physics using the laser as an experimental platform. We demonstrate direct control of the mode-locking state using spectral pulse shaping by incorporating a spatial light modulator at a Fourier plane inside the cavity of an Yb-doped fiber laser. We show that we can halt and restart mode locking, suppress instabilities, induce controlled reversible and irreversible transitions between mode-locking states, and perform advanced pulse shaping while using pulses as short as 40 fs. © 2016 Optical Society of America

The technological importance of passively mode-locked fiber lasers is well recognized [1,2]. In addition, mode locking is of fundamental importance, since it is inherently nonlinear [3–5] and constitutes a non-equilibrium steady state [6]. The same nonlinearity that makes mode locking possible ultimately limits laser performance. In response, researchers have devised numerous ways to manage nonlinearity. Prior to the seminal paper of Ippen and co-workers in 1993 [7], which introduced dispersion management to laser cavities, mode-locked fiber lasers could at best generate several-hundred femtosecond pulses with energies of tens of picojoules. Dispersion management weakens nonlinearity by increasing the average pulse duration. An alternative is to increase the mode area of the fibers [8,9]. Use of microstructured rod-type fibers has allowed much higher powers to be accessed [9]. However, reduction of nonlinearities is limited both in theory, because the instabilities are never eliminated but are merely pushed to higher powers, often at the cost of generation of longer pulses, and in practice, because, e.g., there are practical limits to mode size. A complementary approach involves management of nonlinear effects directly [10], ranging from use of negative (self-defocusing) nonlinearities [10,11] to identification of nonlinearity-resilient pulse propagation schemes. Milestones include demonstration of the wave-breaking-free laser [12] in

2003, the similariton laser in 2004 [13], the all-normal dispersion laser [14] in 2008, supporting dissipative solitons [15], and the soliton–similariton laser [16] in 2010, which is the only laser to date that has two types of nonlinear waves propagating in the cavity [17]. While these developments have led to superior laser performance and unraveled new laser physics, there is currently no possibility of detailed control over the mode-locking states that the lasers support.

Here, we report on direct control of the mode-locking states, nonlinear restructuring of each state, and reversible and irreversible transitions between them, based on algorithmic modulation of the pulse in the spectral domain directly inside the cavity. To this end, we use a spatial light modulator (SLM) positioned in the Fourier plane of a dispersive delay line in a fiber laser cavity. While use of fixed spectral filters to influence mode locking goes back to the 1980s [18], our results rather build on recent demonstrations of SLM-based spectral filtering in picosecond fiber lasers [19,20] since we require dynamic and fully adjustable control; an excellent review is [17]. We now show that we can initiate or halt mode locking, steer the mode-locking state to more favorable but difficult-to-reach states, prevent cw breakthrough instability, automatically improve pulse shape, and generate pulses as short as 40 fs.

To demonstrate our approach, we have replicated the first wave-breaking-free laser [12] and then modified it to include the SLM. We have chosen this laser because it offered an additional challenge. Even though mode-locked operation, once adjusted, was robust, finding that state required laborious adjustment of the waveplates and pump power to limit a persistent cw peak, which could not be completely eliminated. Could we suppress this peak using the SLM only?

A schematic of the experimental setup is shown in Fig. 1. The repetition rate is approximately 40 MHz. The cavity includes an ∼2.3 m long passive fiber corresponding to the lead fibers of two collimators, a 10% coupler for monitoring, and a wavelength division multiplexer (WDM) for pump delivery. The gain fiber is 30 cm long Yb-doped fiber (Yb1200-4/125, nLIGHT). The 980 nm pump diode provides maximum 600 mW power, ∼500 mW of which can be delivered to the gain fiber following losses at pump protection filters and the WDM. The lead fiber of the collimator after the gain fiber is ∼10 cm. After the fiber section, the beam traverses a 30% beam splitter, followed by a
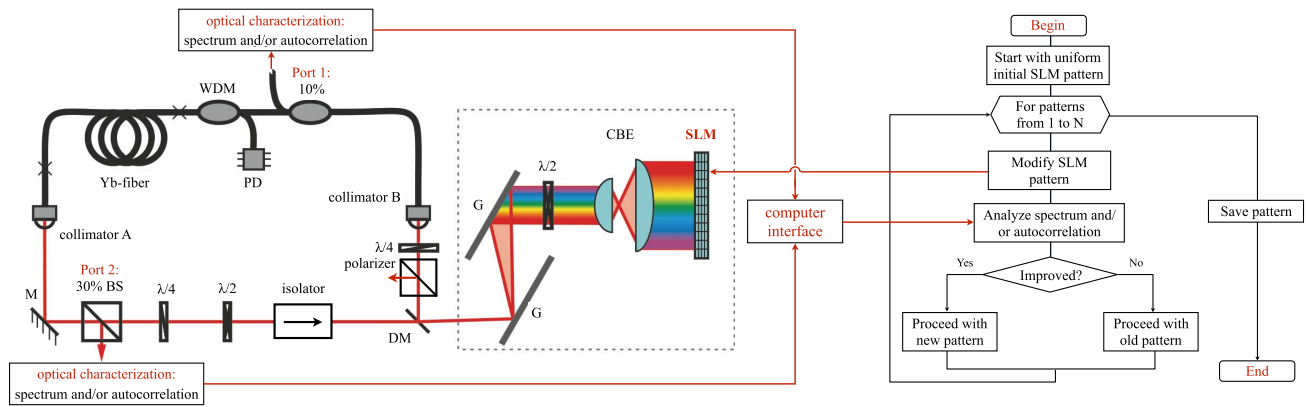
Fig. 1. Schematics of the experimental setup comprising of Yb-doped fiber, wavelength division multiplier (WDM), pump diode (PD), 10% coupler, collimators A and B, 30% non-polarizing beam splitter (BS), $\lambda/2$- and $\lambda/4$ waveplates, polarizing isolator for unidirectional operation, and dispersive delay line with diffraction gratings (G), mirrors (M), D-shaped mirror (DM), cylindrical beam expander (CBE), and spatial light modulator (SLM). The SLM is controlled by a computer algorithm, which takes into account measured optical spectrum or autocorrelation data. The main elements of the quasi-real-time control algorithm are also shown.

quarter- and a half-wave plate, a polarizing beam splitter, which converts polarization rotation into amplitude modulation, a dispersive delay line, and a final quarter-wave plate that converts the beam into elliptical polarization before coupling back into the fiber section. Total cavity dispersion was set to $+4000\ \mathrm{fs}^2$.

The SLM (Pluto, Holoeye) was incorporated by replacing the end mirror of the dispersive delay line. The beam incident on the SLM matrix is spectrally spread along the horizontal direction with a resolution of 25 pixels/nm. Each column of pixels of the SLM matrix imparts a relative phase delay that can electronically be adjusted over the $0 - 2\pi$ range. The beam is optionally expanded by a cylindrical beam expander (expansion ratio of 1:3.2) to better fill the SLM aperture. The grating pair partially acts as a linear polarizer, and it is followed by another polarizer. By including a half-wave plate between the SLM and the grating pair, we convert the spectral phase modulation imparted by the SLM to amplitude modulation. The modulation depth is adjustable through the half-wave plate. The lowest and highest transmissions are set to ∼20% and 64%, respectively. The lower value is set conservatively by the losses that the laser can comfortably tolerate. The upper limit is determined by the losses of the SLM matrix. Transmittance of each spectral element can be independently adjusted to 180 equal levels. Despite the losses of the SLM, typical power after the gain fiber is 180 mW and power coupled back into the fiber section is 13 mW at pump power of 400 mW. This is close to the typical efficiency for similar lasers, implying that the presence of the SLM does not contract the accessible phase space of the laser's operation too much.

The fundamental capability of the SLM to transform a pulse is the same as in its well-known usage outside the cavity [21,22]. However, because of being placed inside the cavity, its role is completely different. The SLM becomes another cavity element that transforms the pulse nonlinearly and dispersively, with the major advantage of this transformation being dynamically reconfigurable. Nevertheless, it is also constrained and cannot be made to impart an arbitrary transformation, because it must comply with the stringent requirement that all changes must balance each other at the end of one round trip [10,23].

For simple tasks, such as disruption of mode locking or preliminary and crude shaping of prominent features in the

spectrum, one can guess the required spectral transmission profile after having acquired some experience. For a more complex operation, the necessary spectral transformation profile is not easy to determine. We have developed an iterative computer algorithm (Fig. 1) to which we can specify various goals, such as reduction of autocorrelation width, maximization of the autocorrelation's peak, or maximization of FWHM (or root mean square, e.g.) of the spectrum. This iterative procedure is capable of testing a large number (of the order of thousands) of transmission profiles in order to maximize a merit function, which is supposed to characterize the desired outcome. For experimental measurement and confirmation, either the optical spectrum or autocorrelation can be used. Overall, this configuration constitutes a quasi-real-time feedback loop among the laser, the SLM, and the controlling computer.

For the sake of simplicity, we now describe a specific implementation of the optimization algorithm that maximizes the FWHM of the spectral bandwidth. Other variants, such as disruption of mode locking (requiring minimization of the spectral FWHM), elimination of a specific feature (by calculating the merit over a limited portion of the spectrum), or maximization of another merit (such as the autocorrelation width) are implemented similarly. Using a single numerical value as merit has obvious limitations, but it allows us to vastly simplify the algorithm and increase the iteration speed. The iterative process itself is primitive, but robust and effective (albeit with some restrictions, discussed below): It scans the spectrum from one edge to the other, experimenting with different phase values for each spectral element. The transmission values are varied by scanning the phase value from $-\pi/16$ to $+\pi/16$ with steps of $\pi/96$ around its previous value. If any change results in an increase of the spectral bandwidth, the value of that spectral element is updated. To minimize erroneous updates due to naturally occurring fluctuations, the FWHM values are first averaged over five measurements, and total measurement takes 50–70 ms. The SLM matrix itself can be updated within 20 ms. Thus, a full readout and reconfiguration cycle lasts about 100 ms. While this is relatively fast, typically thousands of iterations are made. Each optimization ranged from mere seconds or several minutes (for simple tasks) to as much as 3 h for an exhaustive search. We note that both the algorithm and

the data acquisition setup described here constitute a first dem-
onstration and can certainly be vastly improved by sophisticated
algorithms, such as those used in [24].

We first demonstrate the ability to initiate or halt mode lock-
ing, followed by suppression of an instability, and finally by de-
tailed shaping of the spectrum (Fig. 2). We have found that a
transmission profile with a local dip at the central wavelength
of the laser, surrounded by two neighboring, deeper minima [state
1 of Fig. 2(a)], is highly effective in disrupting mode locking with
only ~10% of reduction in transmittance at those wavelengths,
even though the wave plates were adjusted for self-starting mode
locking. To put this value into perspective, we note that the same
cavity could tolerate much higher losses (up to 90% was observed)
in certain waveplate settings [12] when losses were spectrally uni-
form. We repeatedly confirmed that mode locking immediately
restarted after the SLM was set to uniform transmission [or some
other profile, such as state 5 of Fig. 2(a)]. Halting and restarting of
mode locking could be repeated indefinitely at other mode-
locking states that the laser exhibited at different pump power and
waveplate settings. Similarly, when the laser is in a non-self-
starting mode-locking state, mode locking can be initiated by
applying a narrow filter, which is gradually broadened and then
removed.

Next, we show that we can suppress a commonly encountered
instability, namely, formation of a CW peak accompanying a
mode-locked spectrum [state 2 in Fig. 2(a)] when the intracavity
energy exceeds the level a single pulse can hold. Further increases
in nonlinearity lead to a bifurcation; most commonly, the pulse
breaks up into multiple pulses or, less commonly, transitions into
a noise-like state or into a multiwavelength state [5]. Even before
such a bifurcation, the presence of a CW peak leads to an
order-of-magnitude increase in intensity fluctuations of the laser
[25]. To illustrate this, we adjust the pump power and waveplate

settings for a self-starting mode-locked state with an accompany-
ing cw state to be formed when the SLM is set to a flat transmit-
tance profile. We show that by selectively reducing transmission
of its central wavelength, the CW peak can be reduced [state 3 of
Fig. 2(a)], highly suppressed (state 4), and even completely
eliminated (state 5).

The transitions shown in Fig. 2(a) are completely reversible
and indefinitely repeatable. By switching the profile of the
SLM, we can transition among all five states reliably and in either
direction. From the physics point of view [26], irreversible tran-
sitions are most interesting. We can indeed induce irreversible
transitions using the SLM controllably and repeatedly: By turning
the pump off and on, the laser is always placed in the same origi-
nal state, so the experiment can be repeated indefinitely many
times. Upon execution of an SLM pattern sequence, the laser
transitions to a different state. However, upon application of
the time-reversed sequence, unlike the reversible transitions in
Fig. 2(a), the laser ends up at different mode-locking states at each
realization due to fluctuations (noise) present in the system
[Figs. 2(b) and 2(c)]. This setup is ideally suited to test emerging
theories about non-equilibrium systems [27].

A legitimate concern is whether the SLM introduces spurious
optical phase, deteriorating the pulse quality, or excess intensity
noise, both of which may not be discernible from the optical spec-
trum. To check against the former, we dechirped spectra outside
of the cavity using a grating compressor for various cases. We were
able to obtain pulses as short as 40 fs, assuming a Gaussian de-
convolution factor when we optimized for minimum autocorre-
lation width [Fig. 2(d)]. Given the spectral width of 50 nm, the
time–bandwidth product is 0.56, which is within 25% of the
transform limit. The pedestal is likely due to residual third-order
dispersion (TOD) and excess nonlinear phase shift. The second
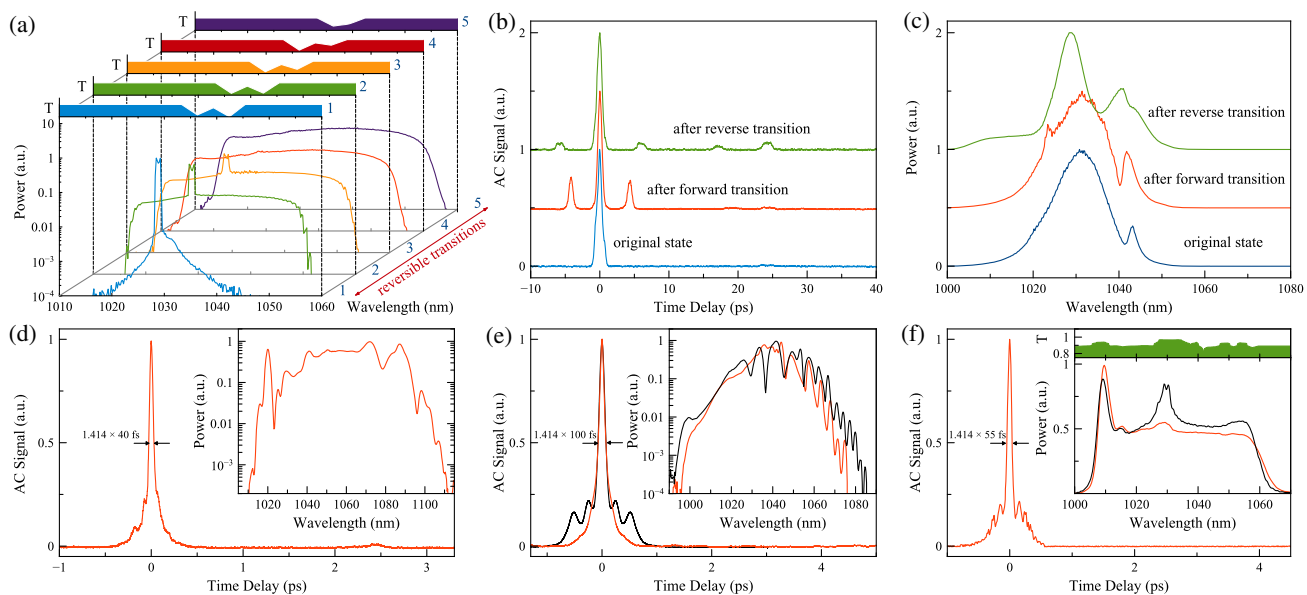possibility is addressed by close-up RF spectrum around the

Fig. 2.   Control of mode-locking states using the SLM. (a) Optical spectra corresponding to reversible transitions from cw to mode locking with cw
peak to pure mode locking. The corresponding spectral filters applied by the SLM are shown at the top of each panel. (b) Autocorrelations and (c) optical
spectra corresponding to repeatable irreversible transitions. (d) Autocorrelation trace of 40 fs long pulses. Inset shows corresponding optical spectrum.
(e) Autocorrelation traces showing SLM-based pedestal removal; inset shows corresponding optical spectra. Black (red) lines before (after) filtering.
(f) Elimination of undesired, characteristic spectral structure for a wave-breaking-free laser operating near its stability limit in terms of pulse energy
[12]. Autocorrelation trace is shown. Inset shows spectra before filtering (black line) and after filtering (red line) along with the filter transmission pattern.

fundamental repetition frequency, which shows at least 90 dB (limited by measurement) suppression of sidebands. Thus, there is no evidence of adverse effects on pulse shape or excess noise due to the SLM.

Finally, we demonstrate use of the SLM for advanced pulse shaping. Our purpose here is to demonstrate the potential, rather than to optimize this specific laser's output. Thus, we provide only generic examples. We first focus on cleaning up the pedestal for an intentionally chosen, highly structured spectrum [Fig. 2(e)]. In our experience, such a spectrum corresponds to the edge of stability of mode locking. The SLM profile we converge to is a simple narrow (6 nm wide) band-stop filter (centered around 1030 nm), which transforms the laser to another, less modulated spectrum. This example succinctly demonstrates that the nonlinearity and periodicity of the cavity means that even a small spectral modulation with a profile that no human would likely guess can have large consequences.

As discussed above, our self-imposed target was to duplicate the hard-to-find mode-locking state that is characteristic of the original wave-breaking-free laser. We duplicate this state as recorded from Port 2 (Fig. 2(f); note the similarity to Fig. 2 of [12]). We focus on suppression of the pesky structure at the center, which contains about ∼20% of the total energy. The structure on the blue edge is a characteristic feature of this mode-locking state, akin to similar structures on all-normal-dispersion lasers [14]. As such, one should not attempt to eliminate it; otherwise, the mode-locking state changes completely. This time, our algorithm converges to a more complex profile [top panel of the inset of Fig. 2(f)], which leads to excellent suppression of this feature, resulting in a spectral width of 50 nm. The corresponding dechirped pulse duration is 55 fs, assuming a Gaussian pulse, where the width and the size of the pedestal are similar to the results in [12]. However, this state is now obtainable using a simple algorithm controlling the SLM. Thus, we have met our original challenge of obtaining a wave-breaking-free laser mode and also eliminating this pesky spectral feature without active human intervention.

We now discuss restrictions of SLM-based control and future perspectives. First, unsurprisingly, the optimization process is more effective when the spectrum to be optimized is taken from a point close to the SLM. Second, our present algorithm has much room for improvement. An interesting future possibility is hybrid control, where modifications would be determined by numerical simulations that take real-time experimental data as input. We have made preliminary attempts in this direction, but at present the process is too slow for practical use. Third, an intracavity SLM may not be desirable for non-scientific applications due to its cost. One can first determine the spectral profile that addresses a specific need using the SLM, after which a custom dielectric filter with corresponding profile can replace the SLM.

In conclusion, we have demonstrated adaptive selection of controlled transitions between and individual restructuring of mode-locking states using an intracavity SLM, including generation of pulses as short as 40 fs with ease. The demonstrations reported here provide merely a glimpse of what is possible. Clearly, various practical applications can be imagined, such as improving laser performance and automated mode locking [24]. We are deeply motivated to use this capability to experimentally investigate bifurcations, reversible and irreversible transitions, by selecting, steering, and even competing various mode-locking states. Such studies can explore collective dynamics of dissipative soliton molecules [15], Casimir-like pulse-to-pulse interactions [28], and ultimately test emerging theories about far-from-equilibrium physics [26,27], where there is an acute lack of experimental systems that are sufficiently well controlled.

†These authors contributed equally.

REFERENCES

1. C. Xu and F. W. Wise, Nat. Photonics **7**, 875 (2013).
2. M. E. Fermann and I. Hartl, Nat. Photonics **7**, 868 (2013).
3. S. Wang, A. Docherty, B. S. Marks, and C. R. Menyuk, J. Opt. Soc. Am. B **31**, 2914 (2014).
4. B. G. Bale, K. Kieu, J. N. Kutz, and F. Wise, Opt. Express **17**, 23137 (2009).
5. J. S. Feehan, F. Ö. Ilday, W. S. Brocklesby, and J. H. V. Price, J. Opt. Soc. Am. B **33**, 1668 (2016).
6. A. Gordon and B. Fischer, Phys. Rev. Lett. **89**, 103901 (2002).
7. K. Tamura, E. P. Ippen, H. A. Haus, and L. E. Nelson, Opt. Lett. **18**, 1080 (1993).
8. M. E. Fermann, Opt. Lett. **23**, 52 (1998).
9. M. Baumgartl, C. Lecaplain, A. Hideur, J. Limpert, and A. Tünnermann, Opt. Lett. **37**, 1640 (2012).
10. F. Ö. Ilday and F. W. Wise, J. Opt. Soc. Am. B **19**, 470 (2002).
11. C. R. Phillips, A. S. Mayer, A. Klenner, and U. Keller, Optica **2**, 667 (2015).
12. F. Ö. Ilday, J. R. Buckley, H. Lim, F. W. Wise, and W. G. Clark, Opt. Lett. **28**, 1365 (2003).
13. F. Ö. Ilday, J. R. Buckley, W. G. Clark, and F. W. Wise, Phys. Rev. Lett. **92**, 213902 (2004).
14. W. Renninger, A. Chong, and F. Wise, Phys. Rev. A **77**, 023814 (2008).
15. P. Grelu and N. Akhmediev, Nat. Photonics **6**, 84 (2012).
16. B. Öktem, C. Ülgüdür, and F. Ö. Ilday, Nat. Photonics **4**, 307 (2010).
17. S. Boscolo, J. Peng, and C. Finot, Appl. Sci. **5**, 1379 (2015).
18. K. L. Schehrer, E. S. Fry, and G. T. Bennett, Appl. Opt. **27**, 1908 (1988).
19. S. Boscolo, C. Finot, H. Karakuzu, and P. Petropoulos, Opt. Lett. **39**, 438 (2014).
20. J. Peng and S. Boscolo, Sci. Rep. **6**, 25995 (2016).
21. D. Yelin, D. Meshulach, and Y. Silberberg, Opt. Lett. **22**, 1793 (1997).
22. A. M. Weiner, Rev. Sci. Instrum. **71**, 1929 (2000).
23. H. A. Haus, IEEE J. Sel. Top. Quantum Electron. **6**, 1173 (2000).
24. U. Andral, R. S. Fodil, F. Amrani, F. Billard, E. Hertz, and P. Grelu, Optica **2**, 275 (2015).
25. I. L. Budunoglu, C. Ülgüdür, B. Öktem, and F. Ö. Ilday, Opt. Lett. **34**, 2516 (2009).
26. C. Jarzynski, Annu. Rev. Condens. Matter Phys. **2**, 329 (2011).
27. J. L. England, Nat. Nanotechnol. **10**, 919 (2015).
28. R. Weill, A. Bekker, V. Smulakovsky, B. Fischer, and O. Gat, Optica **3**, 189 (2016).